IEEE Access
Multidisciplinary ⋮ Rapid Review ⋮ Open Access Journal

Received 24 November 2023, accepted 11 December 2023, date of publication 18 December 2023,
date of current version 28 December 2023.

Digital Object Identifier 10.1109/ACCESS.2023.3343954

RESEARCH ARTICLE

Electrocardiogram Signal Secure Transmission via a Wireless Communication Protocol of Chaotic Systems Based on Adaptive Sliding Mode Control and Disturbance Observer

MINH CHIEN LE[1], VAN NAM GIAP[1], QUANG DICH NGUYEN[1,3], AND SHYH-CHOUR HUANG[2], (Senior Member, IEEE)

[1]School of Electrical and Electronic Engineering, Hanoi University of Science and Technology, Hanoi 100000, Vietnam
[2]Department of Mechanical Engineering, National Kaohsiung University of Science and Technology, Kaohsiung 807618, Taiwan
[3]Institute for Control Engineering and Automation, Hanoi University of Science and Technology, Hanoi 100000, Vietnam

Corresponding authors: Shyh-Chour Huang (shuang@nkust.edu.tw) and Van Nam Giap (nam.giapvan@hust.edu.vn)

This work was supported by the National Science and Technology Council of the Republic of China under Contract NSTC 112-2221-E-992-040.

ABSTRACT This paper presents a new application of the encryption and decryption techniques for securing the electrocardiogram (ECG) signal. The secure communication system (SCS) is embedded two Chen chaotic systems with different initial conditions, which were named master and slave, respectively. An ECG signal is encrypted by using master chaotic system. Which can be sent to the far destination to serving the heath care monitoring process. To obtain the original data, the state of the slave system is used to decrypt the signal. To obtain the goal, the master and slave need to be synchronized. Therefore, to softening the calculation of synchronization control design, the Takagi-Sugeno fuzzy (TSF) was used to remodel the master and slave into the fuzzy format, which are consists of the sublinear systems and fuzzy outer membership functions. Second, the disturbance observer (DOB) was proposed on slave system, which is used to reject the parameters variations and disturbances during the transmission. Third, the sliding mode control (SMC) was designed to synchronize the master and slave systems. Fourth, the stability of SCS is proved based on the Lyapunov condition. Finally, the simulation by using MATLAB software on computer and experiment by using the WIFI microchip ESP8266 were provided to show the power of the proposed methods.

INDEX TERMS Electrocardiogram, secure communication system, Takagi-Sugeno fuzzy, disturbance observer, sliding mode control.

I. INTRODUCTION

Nowadays, the secure communication system (SCS) is more and more important. Especially, in the fourth industrial revolution era, sensor devices around us collect and transmit sensitive information such as personal information, healthy information, location, consumer behavior and so on. The electrocardiogram (ECG) is an important signal in the health care and monitoring process [1]. The ECG can be used for application of the computer aided diagnosis system [1]. The ECG can be used to analyze the sleep time [2], [3]. The driver emotion recognition using ECG was presented in [4]. Together with the development of the industrial devices, the computer aided system for health care processes is growth. Therefore, the security problem is more and more considered in the system. The security of the health care signal was presented in [5]. The encryption and decryption of the ECG signal is presented in [6]. Herein, the secure communication of two wireless devices is presented with application of the secure ECG application. The presented secure communication system is real time operation. The application of wireless secure communication of chaotic systems was presented

The associate editor coordinating the review of this manuscript and approving it for publication was Junggab Son.

in [7]. The SCS of chaotic systems with applications on the electronic circuits can be found in [8], [9], [10], and [11]. The secure of images were presented in [12], [13], [14], [15], and [16]. The secure communication based on microcontroller was presented in [17].

Herein, the Takagi-Sugeno fuzzy (TSF) modeling is used to convert the discrete-time chaotic system into the fuzzy format. The basic concept of the sector nonlinearity method can be found in [18], which was used for convert the chaotic system into the fuzzy model in this paper. The applications of the TSF in secure communication control systems can be found in [19], [20], [21], [22], and [23]. The other applications of TSF in control design can be found in [24], [25], and [26]. In fact, the TSF was used for modeling the master and slave systems (MSSs) for serving the control design online. In the real communication system, MSSs were remained in the original chaotic systems. After obtaining the MSSs in the fuzzy format, the DOB was designed and embedded into the slave side. Which helps the control system robust with external attacks and internal changing.

Herein, the disturbances on public channels were assumed embedded into the slave area. The DOB in this paper is proposed to overcome the illness of the conjunction of the template of disturbance and its first derivative of the previous papers [27], [28], [29], [30]. The DOB of this paper was adaptively designed to cope with the complexity of disturbances. The synchronize control was obtained based on the adaptive SMC. The basic concept of SMC can be found in [31]. Moreover, this paper introduces the adaptive SMC method, which reduces significantly the chattering phenomenon. This has been discussed in [7].

As well-known SMC can be used with the aim of softening the matched disturbances. However, that depends on the reaching gain of the switching control signal. The larger reaching gain coefficient leads the disturbance to be eliminated. However, this also leads to an increase the chattering phenomenon. Hence, the use of a disturbance observer is requested for effective disturbance rejection.

Motivated from the previous papers in the ECG encryption and decryption methods [32] without the consideration of disturbance effects. The proposed synchronization of [33] also ignored the effect of the disturbance. According to the best of the author's knowledge, the number of discussions for real time ECG secure on wireless protocol is minimal. Therefore, the real system of ECG with robustness control is designed. The contributions of this paper are listed below.

1. The mathematical mode of the Chen chaotic system is remodel into the TSF system in the discrete-time domain. This is a first stage of the computation on chips of the control design for SCS.
2. An adaptive DOB was designed to estimate the unwanted signal both on the public channels and variations of parameters on master and slave sides. Together with the DOB, an adaptive SMC was designed to synchronize the master and slave systems.
3. The stability was theoretically verified by using Lyapunov condition.
4. To show the power of the proposed control methods, the simulation of MATLAB software was used to conduct the correction and effectiveness. To enhance the visualization of the power of the proposed method, the experimental study of the wireless secure communication system was used to obtain the goal. The obtained results are good to state that the designed control system is good for secure the ECG data.

The paper consists of the introduction in the first section. The preliminary mathematics were shown in section II. The proposed control methods for SCS are given in the third section. The simulation and experimental studies are given in the fourth section. In the last, conclusion and some concluding remarks of future work are given.

II. PRELIMINARY MATHEMATICS AND PROPOSED THEORY

Herein, the mathematical modeling of the TSF and the basic concept of the proposed DO are given. First, the TSF is given as below.

A. TSF MODELING

First, the nonlinear system is considered:

$$\begin{cases} \dot{\chi} = g^m\{x,u\}\chi + h^m\{x,u\}u \\ y = l^m\{x,u\}\chi \end{cases} \tag{1}$$

where, χ is the state vector of the system with n variable; y is output vector; u is control input; g^m, h^m and l^m are smooth functions of state χ.

According to [18], system (1) can be remodeled as:

$$\begin{cases} \dot{\chi} = \sum_{i=1}^{r} \omega_i(\chi_j)(A_i\chi + B_i u) \\ y = C\chi \end{cases} \tag{2}$$

where

$$\begin{cases} w_0^j(\chi_j) = \dfrac{\chi_{\max}^j - \chi_j(.)}{\chi_{\max}^j - \chi_{\min}^j} \\ w_1^j(\chi_j) = 1 - w_0^j \end{cases} \tag{3}$$

The condition of the state of the nonlinear system (1) is satisfied $\chi_j \in [\chi_{j\min}, \chi_{j\max}]$.

B. CALCULUS IN DISCRETE-TIME DOMAIN

Herein, the basic concepts and properties of the derivative calculus are given.

Definition 1: Simple approximation of the first derivative at time t_k as follows: [34]. Forward differencing:

$$f'(t_k) \approx \frac{f(t_k + h) - f(t_k)}{h} \tag{4}$$

Backward differencing:

$$f'(t_k) \approx \frac{f(t_k) - f(t_k - h)}{h} \tag{5}$$

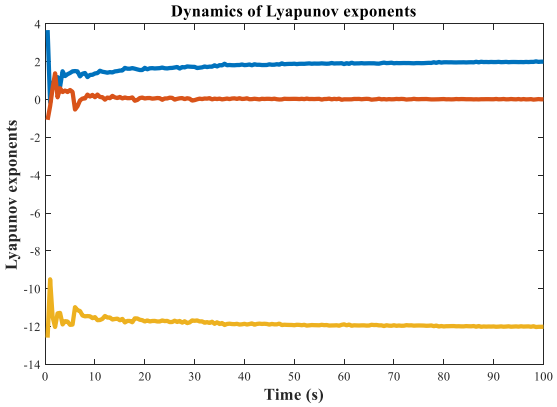

FIGURE 1. Lyapunov exponents of Chen chaotic in discrete time domain.

Central differencing:

$$f'(t_k) \approx \frac{f(t_k + h) - f(t_k - h)}{2h} \tag{6}$$

With h is time step; $t_k = kh$ and $k = 0, 1, 2\ldots$ Therefore, a first-order differential equation in the continuous time domain as follows:

$$\dot{y}(t) = f(t) \tag{7}$$

can be represented in the discrete time domain as follows:

$$y(t_{k+1}) = y(t_k) + hf(t_k) \tag{8}$$

C. MASTER AND SLAVE MODELING

Chen's chaotic system of this paper is reused from [35], in the continuous time domain:

$$\begin{cases} \dfrac{dx}{dt} = -ax(t) + ay(t) \\ \dfrac{dy}{dt} = -\tau x(t) + cy(t) - x(t)z(t) \\ \dfrac{dz}{dt} = x(t)y(t) - bz(t) \end{cases} \tag{9}$$

With $a = 35,\ b = 3,\ c = 28,\ \tau = a - c$. System (9) can be converted into the discrete time domain such as follows:

$$\begin{cases} x(t_{k+1}) = x(t_k) + h \times [-ax(t_k) + ay(t_k)] \\ y(t_{k+1}) = y(t_k) + h \times [-\tau x(t_k) + cy(t_k) - x(t_k)z(t_k)] \\ z(t_{k+1}) = z(t_k) + h \times [x(t_k)y(t_k) - bz(t_k)] \end{cases} \tag{10}$$

To show the correction of the continuous time to discrete time chaotic system, the Lyapunov exponent of the converted system is shown in Figure 1.

Figure 1 shown the Lyapunov exponents of Chen chaotic in discrete time domain follow (10) with step time $h = 0.001s$ and initial conditions $x(0) = 0.15; y(0) = 0.25; z(0) = -0.5$. The Jacobian matrix is $J = \begin{bmatrix} -35 & 35 & 0 \\ -7 - 20z & 28 & -20x \\ 5y & 5x & -3 \end{bmatrix}$.

MATLAB was used to get the Dynamics of Lyapunov exponents. The Lyapunov exponents are $L_1 = 2.015; L_2 = 0; L_3 = -12.013$. The fractal dimension of reduced scales chaotic system is 2.168. The equivalent points are $\lambda_1 = \begin{bmatrix} 0 \\ 0 \\ 0 \end{bmatrix}$, $\lambda_2 = \begin{bmatrix} -1012.7 \\ 27897j \\ 28328 \end{bmatrix}$, and $\lambda_3 = \begin{bmatrix} 1012.7 \\ -27897j \\ 28328 \end{bmatrix}$. Applying the TSF modeling with the sector nonlinearity method to convert the system (10) into the fuzzy model yields

$$\chi(t_{k+1}) = \sum_{i=1}^{2} \omega_i \{\chi(t_k)\} A_i \chi(t_k) + H(t_k) \tag{11}$$

where $\chi(t_{k+1}) = \left[x(t_{k+1})\ y(t_{k+1})\ z(t_{k+1})\right]^T$ is state vector. The weighting function $\omega_i \{\chi(t_k)\}$ can be calculated as:

$$\begin{cases} \omega_1(\chi(t_k)) = \dfrac{x_{\max} - x(t_k)}{x_{\max} - x_{\min}} \\ \omega_2(\chi(t_k)) = \dfrac{x_{\max} + x(t_k)}{x_{\max} - x_{\min}} \end{cases} \tag{12}$$

with $x(t_k) \in [x_{\min}, x_{\max}]$. Approximated matrices $A_i \in R^{3\times 3}$ are:

$$\begin{aligned} A_1 &= h \times \begin{bmatrix} -a & a & 0 \\ -\tau & c & -x_{\min} \\ 0 & x_{\min} & -b \end{bmatrix}; \\ A_1 &= h \times \begin{bmatrix} -a & a & 0 \\ -\tau & c & -x_{\max} \\ 0 & x_{\max} & -b \end{bmatrix} \end{aligned} \tag{13}$$

The matrix $H(t_k) \in R^{3\times 1}$ is:

$$H(t_k) = \begin{bmatrix} x(t_k) \\ y(t_k) \\ z(t_k) \end{bmatrix} \tag{14}$$

With the selected parameters $a,\ b,\ c$, $x_{\min} = -100$, and $x_{\max} = 100$, system (10) with fully consideration of the uncertain terms for master is as follows:

$$\begin{cases} x_m(t_{k+1}) = x_m(t_k) + h \\ \times [-(a + \Delta a_m)x_m(t_k) + (a + \Delta a_m)y_m(t_k)] \\ y_m(t_{k+1}) = y_m(t_k) + h \\ \times \begin{bmatrix} -(\tau + \Delta\tau_m)x_m(t_k) + (c + \Delta c)y_m(t_k) \\ -x_m(t_k)z_m(t_k) \end{bmatrix} \\ z_m(t_{k+1}) = z_m(t_k) + h \\ \times [x_m(t_k)y_m(t_k) - (b + \Delta b)z_m(t_k)] \end{cases} \tag{15}$$

where m is mark of master. Δa_m, Δb_m, Δc_m are variations of the parameters.

Therefore, master system can be described as

$$\chi_m(t_{k+1}) = \sum_{i=1}^{2} \omega_{mi} \{\chi_m(t_k)\} A_i \chi_m(t_k) + H_m(t_k) + Dd_m(t_k) \tag{16}$$

where $d_m(t_k) = \left[d_{mx}(t_k)\ d_{my}(t_k)\ d_{mz}(t_k)\right]^T$ is the uncertainty of the master system. Matrix D is an 3×3 identity matrix. The system can work if the assumption 1 can be guaranteed.

Assumption 1: The uncertainty of each axis need to be bounded as follows: $|d_{mx}(t_k)| \leq \varepsilon_x$, $|d_{my}(t_k)| \leq \varepsilon_y$, and $|d_{mz}(t_k)| \leq \varepsilon_z$. Where ε_x, ε_y and ε_z are positively defined.

System (10) with fully consideration of the uncertain terms for slave is as follows:

$$\begin{cases} x_s(t_{k+1}) = x_s(t_k) + h \\ \times \begin{bmatrix} -(a+\Delta a_s)x_s(t_k) + (a+\Delta a_s)y_s(t_k) \\ +u_x(t_k) + l_x(t_k) \end{bmatrix} \\ y_s(t_{k+1}) = y_s(t_k) + h \\ \times \begin{bmatrix} -(\tau+\Delta\tau_s)x_s(t_k) + (c+\Delta c)y_s(t_k) \\ -x_s(t_k)z_s(t_k) + u_y(t_k) + l_y(t_k) \end{bmatrix} \\ z_s(t_{k+1}) = z_s(t_k) + h \\ \times \begin{bmatrix} x_s(t_k)y_s(t_k) - (b+\Delta b)z_s(t_k) \\ +u_z(t_k) + l_z(t_k) \end{bmatrix} \end{cases} \tag{17}$$

where s is marked for representing the slave. Δa_m, Δb_m, Δc_m are variations of the parameters. $l_x(t_k)$, $l_y(t_k)$, $l_z(t_k)$ are disturbance signals on each axis. $u_x(t_k)$, $u_y(t_k)$, $u_z(t_k)$ are control signals on each axis. Therefore, master system can be described as:

$$\chi_s(t_{k+1}) = \sum_{i=1}^{2} \omega_{si} \{\chi_s(t_k)\} A_i \chi_s(t_k) + H_s(t_k) + Bu(t_k) + Dd_s(t_k) \tag{18}$$

where $d_s(t_k) = \left[d_{sx}(t_k)\ d_{sy}(t_k)\ d_{sz}(t_k) \right]^T$ is the disturbance and uncertainty of the slave system. The system can work if the assumption 2 can be guaranteed.

Assumption 2: The disturbance and uncertainty of each axis need to be bounded as follows: $|d_{sx}(t_k)| \leq \theta_x$, $|d_{sy}(t_k)| \leq \theta_y$, and $|d_{sz}(t_k)| \leq \theta_z$. Where θ_x, θ_y and θ_z are positively defined.

III. PROPOSED APPROACH

To design the SMC and DO for the SCS, the definition of the tracking error and some disturbance terms are given. We have

$$\begin{cases} e_x(t_{k+1}) = x_m(t_{k+1}) - x_s(t_{k+1}) \\ e_y(t_{k+1}) = y_m(t_{k+1}) - y_s(t_{k+1}) \\ e_z(t_{k+1}) = z_m(t_{k+1}) - z_s(t_{k+1}) \end{cases} \tag{19}$$

and

$$\begin{aligned} e(t_{k+1}) &= \chi_m(t_{k+1}) - \chi_s(t_{k+1}) \\ &= \sum_{i=1}^{2} \omega_{mi} \{\chi_m(t_k)\} A_i \chi_m(t_k) + H_m(t_k) + Dd_m(t_k) \\ &\quad - \left[\sum_{i=1}^{2} \omega_{si} \{\chi_s(t_k)\} A_i \chi_s(t_k) + H_s(t_k) \right. \\ &\quad \left. + Bu(t_k) + Dd_s(t_k) \right] \end{aligned} \tag{20}$$

By referring $Dd_m(t_k) - Dd_s(t_k) = D\bar{d}(t_k)$. Eq. (20) can be written as follows:

$$\begin{aligned} e(t_{k+1}) &= \sum_{i=1}^{2} \omega_{mi} \{\chi_m(t_k)\} A_i \chi_m(t_k) + H_m(t_k) \\ &\quad - \left[\sum_{i=1}^{2} \omega_{si} \{\chi_s(t_k)\} A_i \chi_s(t_k) + H_s(t_k) + Bu(t_k) \right] \\ &\quad + D\bar{d}(t_k) \end{aligned} \tag{21}$$

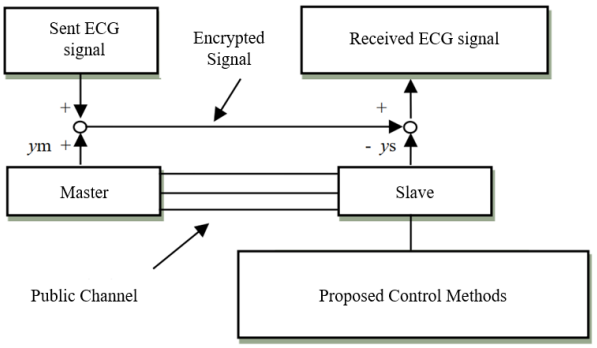

FIGURE 2. The proposed control methods for SCS of ECG signal.

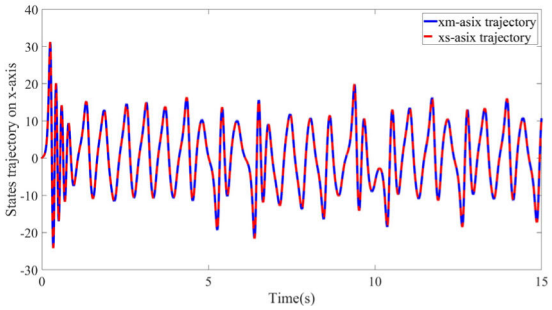

(a)

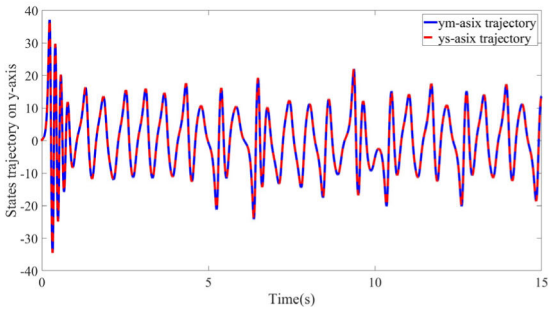

(b)

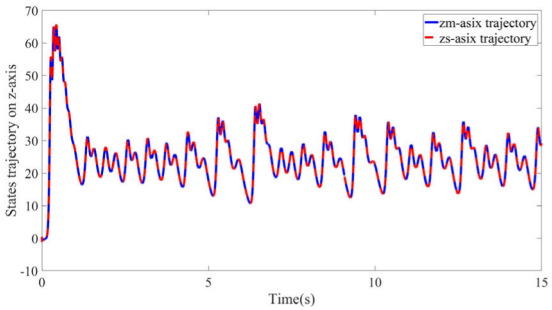

(c)

FIGURE 3. States of the MSSs: (a) x_m and x_s, (b) y_m and y_s, and (c) z_m and z_s.

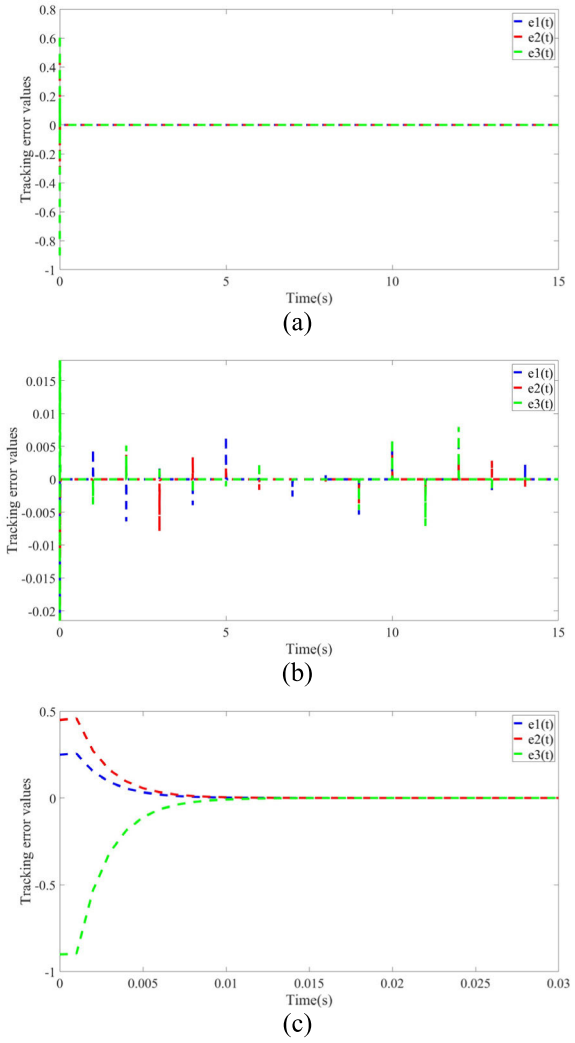

FIGURE 4. Tracking errors: (a) tracking errors without tested disturbance, (b) tracking errors with tested disturbance (c) tracking errors in the first 0.03(s).

A. SLIDING MODE CONTROL FOR SCS

First, the sliding mode surface is designed by:

$$s(t_k) = e(t_k) + \lambda e(t_{k-1}) \tag{22}$$

where $\lambda = \begin{bmatrix} \lambda_x & 0 & 0 \\ 0 & \lambda_y & 0 \\ 0 & 0 & \lambda_z \end{bmatrix}$ is the matrix of sliding surface. To calculate the equivalent control signal, we need consider the system in steady-state. It means the effect of disturbance is not considered. The equivalent control signal, which maintain the system to stay on the sliding mode surface:

$$\begin{cases} s(t_{k+1}) = 0 \\ \bar{d}(t_{k+1}) = 0 \end{cases} \tag{23}$$

Therefore

$$e(t_{k+1}) + \lambda e(t_k) = 0 \tag{24}$$

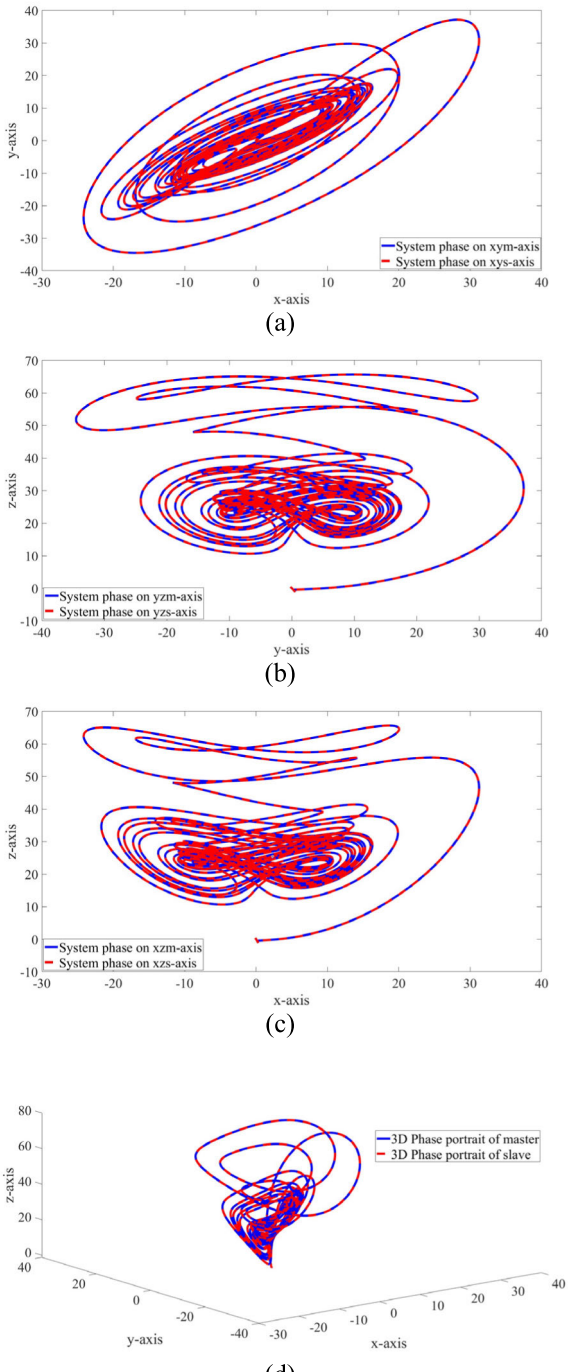

FIGURE 5. Phases of the MSSs: (a) yx-axes, (b) zy-axes, (c) zx-axes, and (d) 3D phase portrait.

Eq. (24) can be written as follows:

$$\sum_{i=1}^{2} \omega_{mi} \{\chi_m(t_k)\} A_i \chi_m(t_k) + H_m(t_k) - \left[\sum_{i=1}^{2} \omega_{si} \{\chi_s(t_k)\} A_i \chi_s(t_k) + H_s(t_k) + Bu(t_k) \right] + \lambda e(t_k) = 0 \tag{25}$$

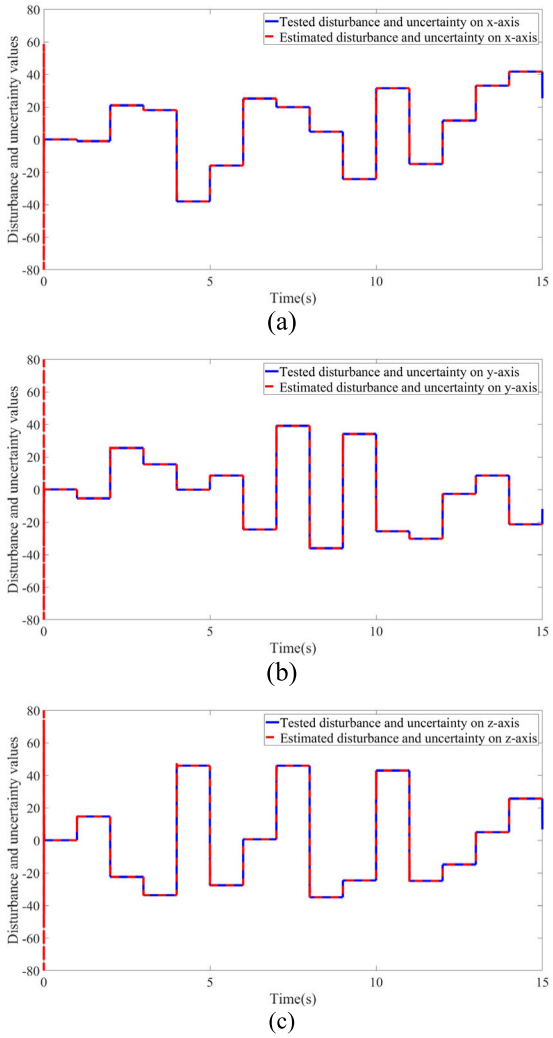

FIGURE 6. Tested and estimated disturbances on three axes: (a) on x-axis, (b) on y-axis, and (c) on z-axis.

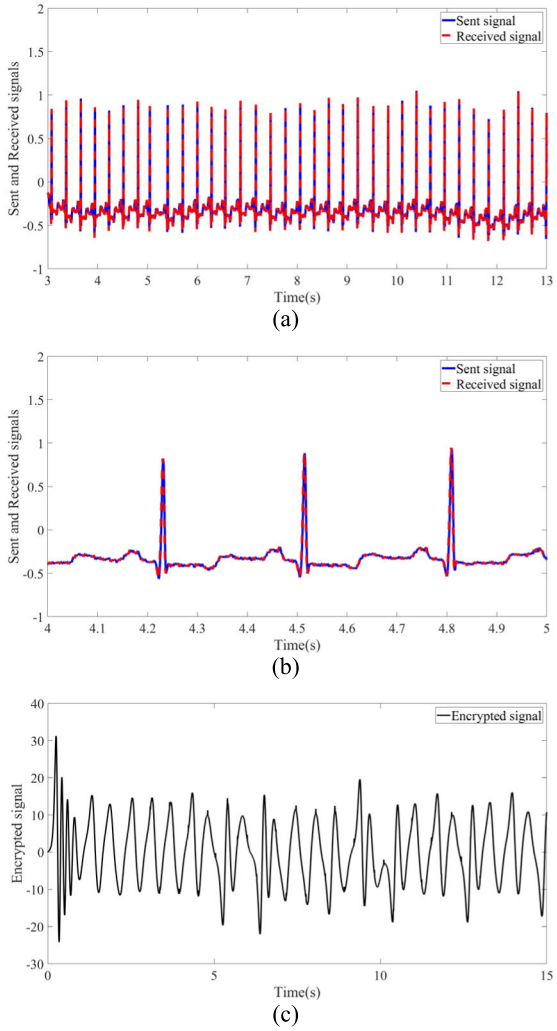

FIGURE 7. Sent and received signal: (a) Sent and received signal in 10(s), (b) Sent and received signal in 1(s), (c) Encrypted signal.

or

$$Bu(t_k) = \sum_{i=1}^{2} \omega_{mi} \{\chi_m(t_k)\} A_i \chi_m(t_k) + H_m(t_k) - \left[\sum_{i=1}^{2} \omega_{si} \{\chi_s(t_k)\} A_i \chi_s(t_k) + H_s(t_k)\right] + \lambda e(t_k) \quad (26)$$

Therefore, the equivalent control of $x-$ axis is as follows:

$$u_{eqx}(t_k) = \begin{bmatrix} 1 & 0 & 0 \end{bmatrix} \sum_{i=1}^{2} \omega_{mi} \{\chi_m(t_k)\} A_i \chi_m(t_k) + H_m(t_k) - \left[\sum_{i=1}^{2} \omega_{si} \{\chi_s(t_k)\} A_i \chi_s(t_k) + H_s(t_k)\right] + \lambda_x e_x(t_k) \quad (27)$$

The equivalent control of $y-$ axis is as follows:

$$u_{eqy}(t_k) = \begin{bmatrix} 0 & 1 & 0 \end{bmatrix} \sum_{i=1}^{2} \omega_{mi} \{\chi_m(t_k)\} A_i \chi_m(t_k) + H_m(t_k) - \left[\sum_{i=1}^{2} \omega_{si} \{\chi_s(t_k)\} A_i \chi_s(t_k) + H_s(t_k)\right] + \lambda_y e_y(t_k) \quad (28)$$

And the equivalent control of $z-$ axis is:

$$u_{eqz}(t_k) = \begin{bmatrix} 0 & 0 & 1 \end{bmatrix} \sum_{i=1}^{2} \omega_{mi} \{\chi_m(t_k)\} A_i \chi_m(t_k) + H_m(t_k) - \left[\sum_{i=1}^{2} \omega_{si} \{\chi_s(t_k)\} A_i \chi_s(t_k) + H_s(t_k)\right] + \lambda_z e_z(t_k) \quad (29)$$

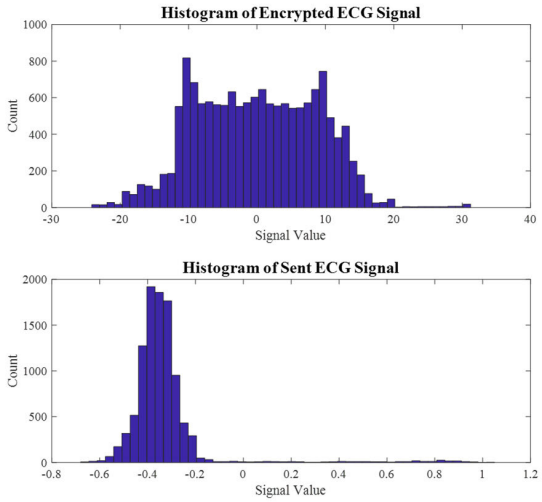

FIGURE 8. Histogram charts compare between encrypted ECG signal and Sent ECG Signal.

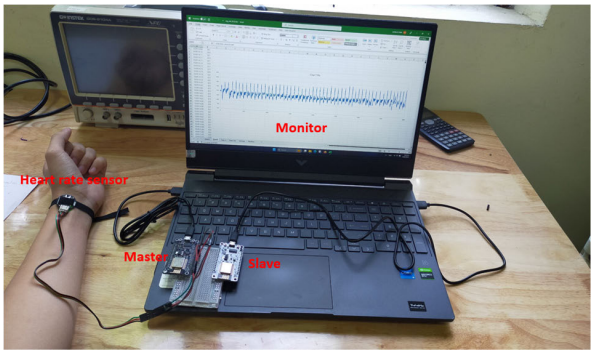

FIGURE 9. Experimental setup.

This paper used the *sign* function to construct the switching control value and chattering will be reduced significantly by an adaptive control. First, the switching control of $x-$ axis is given by:

$$u_{swx}(t_k) = \hat{k}_x sign\{s_x(t_k)\} \tag{30}$$

where $\hat{k}_x$ is the reaching gain for x- axis, achieved by following adaptive law of

$$\hat{k}_x = k_x \left| e_x(t_k) \right| \tag{31}$$

The switching control of $y-$ axis is given by:

$$u_{swy}(t_k) = \hat{k}_y sign\{s_y(t_k)\} \tag{32}$$

where $\hat{k}_y$ is the reaching gain for y- axis, achieved by following adaptive law of

$$\hat{k}_y = k_y \left| e_y(t_k) \right| \tag{33}$$

The switching control of $z-$ axis is given by:

$$u_{swz}(t_k) = \hat{k}_z sign\{s_z(t_k)\} \tag{34}$$

where $\hat{k}_z$ is the reaching gain for z- axis, achieved by following adaptive law of

$$\hat{k}_z = k_z \left| e_z(t_k) \right| \tag{35}$$

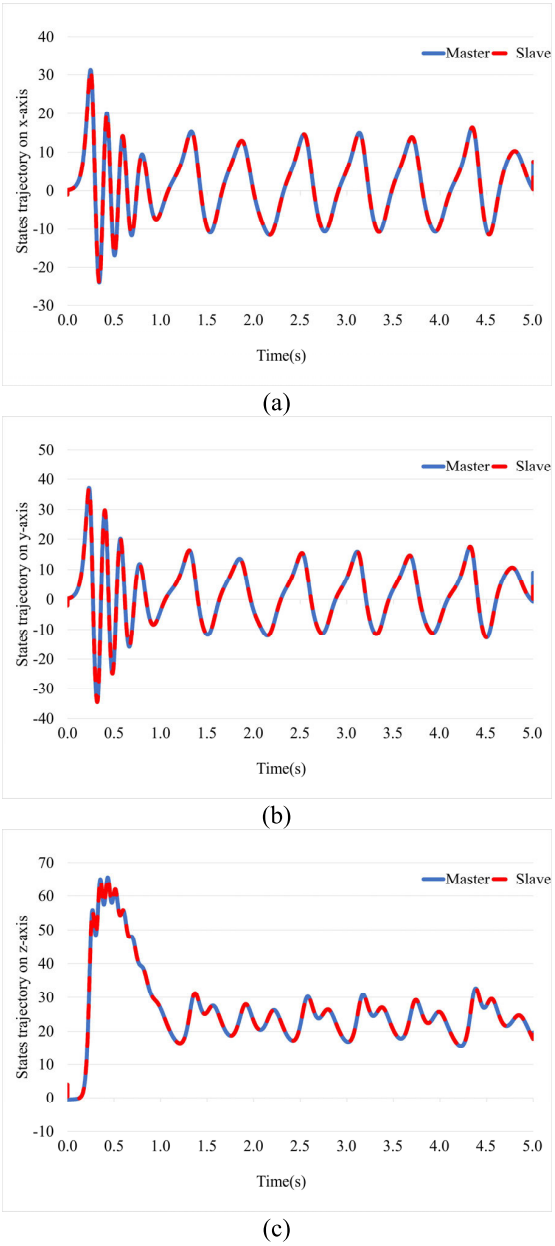

FIGURE 10. States of the MSSs: (a) x_m and x_s, (b) y_m and y_s, and (c) z_m and z_s.

B. DISTURBANCE OBSERVER FOR SCS

The uncertainty of master system and perturbations of slave system together with the attack signals on the public channels can be calculated by:

$$\begin{cases} Dd_m(t_k) = \chi_m(t_{k+1}) \\ \quad - \left[\sum_{i=1}^{2} \omega_{mi} \left\{ \chi_m(t_k) \right\} A_i \chi_m(t_k) + H_m(t_k) \right] \\ Dd_s(t_k) = \chi_s(t_{k+1}) \\ \quad - \left[\sum_{i=1}^{2} \omega_{si} \left\{ \chi_s(t_k) \right\} A_i \chi_s(t_k) + H_s(t_k) \right. \\ \quad \left. + Bu(t_k) + D\hat{d}(t_k) \right] \end{cases} \tag{36}$$

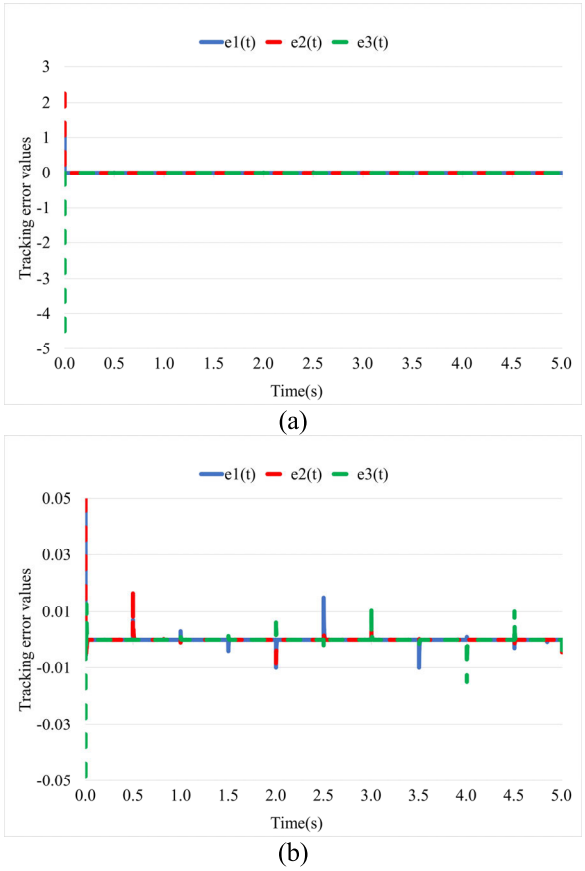

FIGURE 11. The tracking errors: (a) tracking errors without disturbances and (b) tracking errors with disturbances.

where, $\hat{d}(t_k)$ is the proposed DO for SCS. Therefore,

$$\begin{aligned} D\bar{d}(t_k) &= \chi_m(t_{k+1}) - \chi_s(t_{k+1}) \\ &+ \left[\begin{array}{l} \sum_{i=1}^{2} \omega_{si} \{\chi_s(t_k)\} A_i \chi_s(t_k) + H_s(t_k) \\ + Bu(t_k) + D\hat{d}(t_k) \end{array} \right] \\ &- \left[\sum_{i=1}^{2} \omega_{mi} \{\chi_m(t_k)\} A_i \chi_m(t_k) + H_m(t_k) \right] \end{aligned} \quad (37)$$

When the master and slave are synchronized, the $\chi_m(t_{k+1})$ is equal to $\chi_s(t_{k+1})$. It means:

$$\begin{aligned} D\bar{d}(t_k) &= \sum_{i=1}^{2} \omega_{si} \{\chi_s(t_k)\} A_i \chi_s(t_k) \\ &+ H_s(t_k) + Bu(t_k) + D\hat{d}(t_k) \\ &- \left[\sum_{i=1}^{2} \omega_{mi} \{\chi_m(t_k)\} A_i \chi_m(t_k) + H_m(t_k) \right] \end{aligned} \quad (38)$$

The error of estimated and real disturbance is calculated as follows:

$$D\tilde{d}(t_k) = \sum_{i=1}^{2} \omega_{si} \{\chi_s(t_k)\} A_i \chi_s(t_k) + H_s(t_k) + Bu(t_k)$$

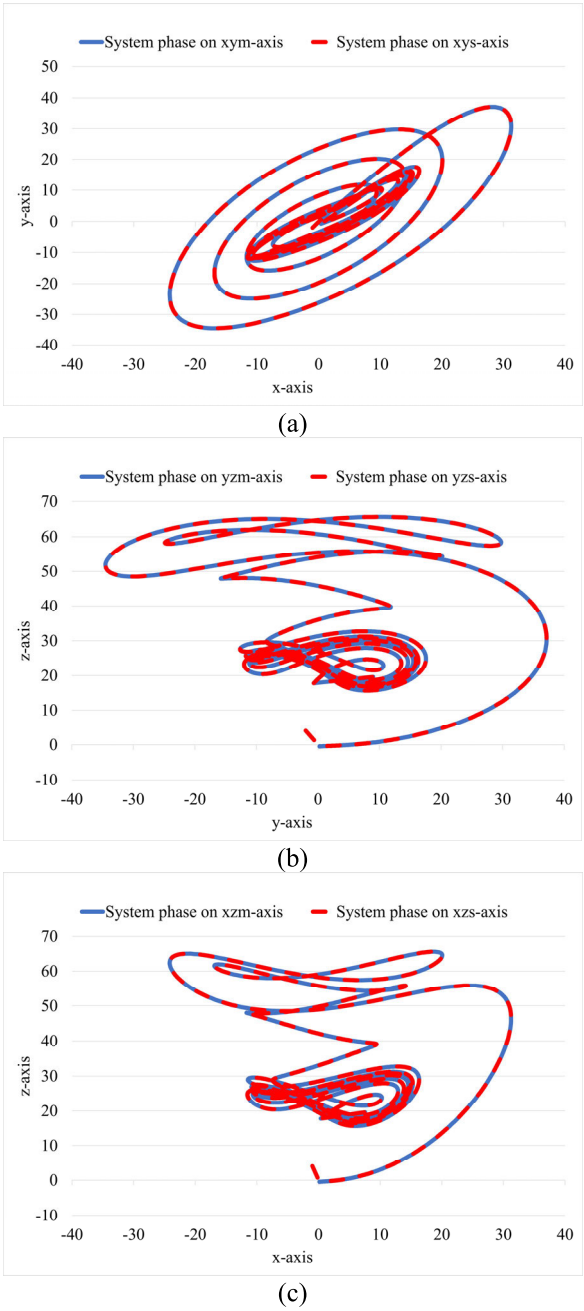

FIGURE 12. Phase of master and slave systems.

$$- \left[\sum_{i=1}^{2} \omega_{mi} \{\chi_m(t_k)\} A_i \chi_m(t_k) + H_m(t_k) \right] \quad (39)$$

The adaptive DO for of this paper is proposed as follows:

$$\hat{d}(t_k) = \bar{d}(t_k) + \hat{k}_d \tilde{d}(t_{k-1}) \quad (40)$$

Therefore, the adaptive DO for x- axis is given by (41), as shown at the bottom of page 10, where $\hat{k}_{dx}$ is the DO gain for x- axis, achieved by following adaptive law such as

$$\hat{k}_{dx} = k_{dx} \left| \tilde{d}_x(t_{k-1}) \right| \quad (42)$$

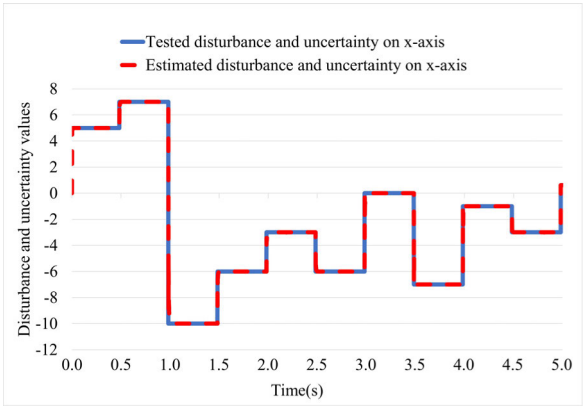

(a)

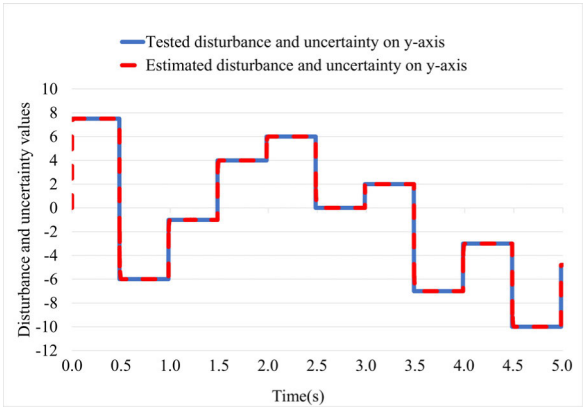

(b)

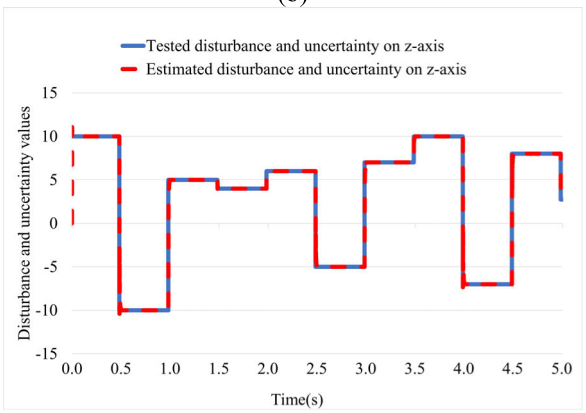

(c)

FIGURE 13. Performance of the proposed DOB: (a) performance on x-axis, (b) performance on y-axis, and (c) performance on z-axis.

The adaptive DO for y- axis is given by (43), as shown at the bottom of the next page, where $\hat{k}_{dy}$ is the DO gain for y- axis, achieved by following adaptive law such as

$$\hat{k}_{dy} = k_{dy} \left| \tilde{d}_y(t_{k-1}) \right| \tag{44}$$

The adaptive DO for z- axis is given by (45), as shown at the bottom of the next page, where $\hat{k}_{dz}$ is the DO gain for z- axis, achieved by following adaptive law such as

$$\hat{k}_{dz} = k_{dz} \left| \tilde{d}_z(t_{k-1}) \right| \tag{46}$$

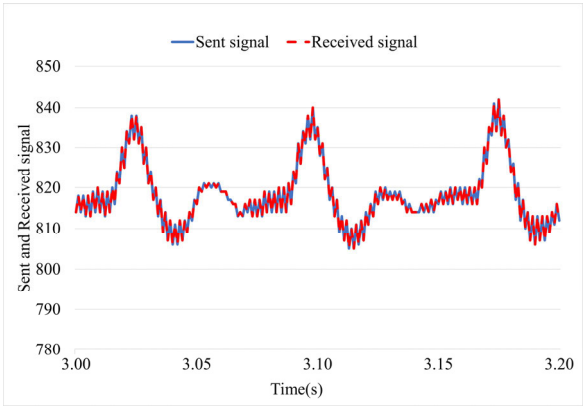

(a)

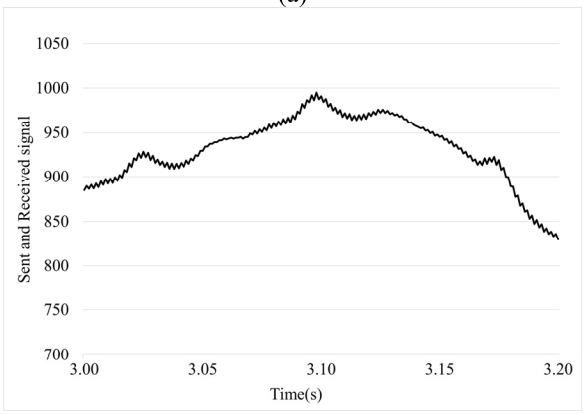

(b)

FIGURE 14. Sent and received signal: (a) Sent and received signal in 0.2(s), (b) Encrypted signal.

Here, D_{1j}, D_{2j}, D_{3j} are row 1, 2, 3 matrix of identity matrix D, respectively.

Remark 1: Eq. (40) at the time t_{k+1} is

$$\hat{d}(t_{k+1}) = \bar{d}(t_{k+1}) + \hat{k}_d \tilde{d}(t_k) \tag{47}$$

or

$$\tilde{d}(t_{k+1}) = -\hat{k}_d \tilde{d}(t_k) \tag{48}$$

C. STABILITY ANALYSIS

The Lyapunov condition is used here to give the proof of stability for whole SCS. The Lyapunov candidate is selected as follows:

$$V\left[s(t_k), \tilde{d}(t_k)\right] = V\left[s(t_k)\right] + V\left[\tilde{d}(t_k)\right] \tag{49}$$

Herein,

$$V\left[s(t_k)\right] = s_x^2(t_k) + s_y^2(t_k) + s_z^2(t_k) \tag{50}$$

By taking derivative for Eq. (50) using the theorem 1 in discrete time yields

$$\dot{V}\left[s(t_k)\right] = \frac{V\left[s(t_{k+1})\right] - V\left[s(t_k)\right]}{h} \tag{51}$$

or

$$\dot{V}\left[s(t_k)\right] = \frac{s^2(t_{k+1}) - s^2(t_k)}{h} \tag{52}$$

From the Section III, it is easily attainable that $s(t_{k+1}) = -\hat{k}sign\left[s(t_k)\right]$. It means:

$$\dot{V}\left[s(t_k)\right] = \frac{\hat{k}_x^2 - s_x^2(t_k)}{h} + \frac{\hat{k}_y^2 - s_y^2(t_k)}{h} + \frac{\hat{k}_z^2 - s_z^2(t_k)}{h} \tag{53}$$

with $\hat{k} = k\left|e(t_k)\right|$ and $s(t_k) = e(t_k) + \lambda e(t_{k-1})$. The initial reaching gain k should be selected to let $\dot{V}\left[s(t_k)\right] < 0$ with $s(t_k) \neq 0$.
and

$$V\left[\tilde{d}(t_k)\right] = \tilde{d}_x^2(t_k) + \tilde{d}_y^2(t_k) + \tilde{d}_z^2(t_k) \tag{54}$$

By taking derivative for Eq. (54) using the definition 1 in discrete time yields

$$\dot{V}\left[\tilde{d}(t_k)\right] = \frac{\tilde{d}_x^2(t_{k+1}) - \tilde{d}_x^2(t_k)}{h} + \frac{\tilde{d}_y^2(t_{k+1}) - \tilde{d}_y^2(t_k)}{h} + \frac{\tilde{d}_z^2(t_{k+1}) - \tilde{d}_z^2(t_k)}{h} \tag{55}$$

or

$$\dot{V}\left[d(t_k)\right] = \frac{\hat{k}_{dx}^2\tilde{d}_x^2(t_k) - \tilde{d}_x^2(t_k)}{h} + \frac{\hat{k}_{dy}^2\tilde{d}_y^2(t_k) - \tilde{d}_y^2(t_k)}{h} + \frac{\hat{k}_{dz}^2\tilde{d}_z^2(t_k) - \tilde{d}_z^2(t_k)}{h} \tag{56}$$

The initial reaching gain k_d should be selected to let $\dot{V}\left[d(t_k)\right] \leq 0$ with.

This completes the proof.

IV. AN ILLUSTRATIVE EXAMPLE

Herein, two illustrative examples are given to show the power of the proposed control methods for securing the ECG signal. The structure of the proposed method for the SCS is illustrated in Figure 2.

$$\hat{d}_x(t_k) = D_{1j}\left\{\begin{array}{l}\sum_{i=1}^{2}\omega_{si}\left\{\chi_s(t_k)\right\}A_i\chi_s(t_k) + H_s(t_k) + Bu(t_k) \\ +D\hat{d}(t_k) \; - \left[\sum_{i=1}^{2}\omega_{mi}\left\{\chi_m(t_k)\right\}A_i\chi_m(t_k) + H_m(t_k)\right]\end{array}\right\} + \hat{k}_{dx}D_{1j}\left\{\begin{array}{l}\sum_{i=1}^{2}\omega_{si}\left\{\chi_s(t_{k-1})\right\}A_i\chi_s(t_{k-1}) + H_s(t_{k-1}) + Bu(t_{k-1}) \\ -\left[\sum_{i=1}^{2}\omega_{mi}\left\{\chi_m(t_{k-1})\right\}A_i\chi_m(t_{k-1}) + H_m(t_{k-1})\right]\end{array}\right\} \tag{41}$$

$$\hat{d}_y(t_k) = D_{2j}\left\{\begin{array}{l}\sum_{i=1}^{2}\omega_{si}\left\{\chi_s(t_k)\right\}A_i\chi_s(t_k) + H_s(t_k) + Bu(t_k) \\ +D\hat{d}(t_k) - \left[\sum_{i=1}^{2}\omega_{mi}\left\{\chi_m(t_k)\right\}A_i\chi_m(t_k) + H_m(t_k)\right]\end{array}\right\} + \hat{k}_{dy}D_{2j}\left\{\begin{array}{l}\sum_{i=1}^{2}\omega_{si}\left\{\chi_s(t_{k-1})\right\}A_i\chi_s(t_{k-1}) + H_s(t_{k-1}) + Bu(t_{k-1}) \\ -\left[\sum_{i=1}^{2}\omega_{mi}\left\{\chi_m(t_{k-1})\right\}A_i\chi_m(t_{k-1}) + H_m(t_{k-1})\right]\end{array}\right\} \tag{43}$$

$$\hat{d}_z(t_k) = D_{3j}\left\{\begin{array}{l}\sum_{i=1}^{2}\omega_{si}\left\{\chi_s(t_k)\right\}A_i\chi_s(t_k) + H_s(t_k) + Bu(t_k) \\ +D\hat{d}(t_k) - \left[\sum_{i=1}^{2}\omega_{mi}\left\{\chi_m(t_k)\right\}A_i\chi_m(t_k) + H_m(t_k)\right]\end{array}\right\} + \hat{k}_{dz}D_{3j}\left\{\begin{array}{l}\sum_{i=1}^{2}\omega_{si}\left\{\chi_s(t_{k-1})\right\}A_i\chi_s(t_{k-1}) + H_s(t_{k-1}) + Bu(t_{k-1}) \\ -\left[\sum_{i=1}^{2}\omega_{mi}\left\{\chi_m(t_{k-1})\right\}A_i\chi_m(t_{k-1}) + H_m(t_{k-1})\right]\end{array}\right\} \tag{45}$$

A. SIMULATION STUDY

Simulation study by using MATLAB code on the computer with CPU Intel(R) Core(TM) i5-12450H, RAM 16GB. The parameters of the proposed control scheme in the simulation study are as follows: total time $t = 15s$ with time step $h = 0.001s$; The initial states of master chaotic system are $x_m(0) = 0.15, y_m(0) = 0.25, z_m(0) = -0.5$; The initial states of slave chaotic system are $x_s(0) = -0.1, y_s(0) = -0.2, z_m(0) = 0.4$; The damping coefficients of SMC: $\lambda_x = 0.5, \lambda_y = 0.5, \lambda_z = 0.5$; The initial reaching gain of SMC: $k_x = 300, k_y = 300, k_z = 800$; The initial gain of DO: $k_{dx} = 0.5, k_{dy} = 0.5, k_{dz} = 0.5$. The performance of the proposed method is shown in Figures. 3-7. First, the states of master and slave are shown in Fig. 3. The tracking errors are all small. To show the power of the proposed control method, the states of the MSSs are firstly shown.

The settling time of three axes is approximately 0.015s. In the first period, the vibrations of convergence appeared. Afterward, the tracking errors rapidly converged into zero. When system was at the time 0.5 (s), the tracking errors is less than 1×10^{-11}. Starting from 1 (s), tested disturbance with random values from -50 to 50, which changes every second was added to slave system. The maximum error when tested disturbance is added is 7×10^{-3}. The tracking errors of the tested studies with and without the disturbances are shown in Figure 4.

To show the correction of the designed secure communication system, the phases of the master and slave after synchronized are shown in Figure. 5. Which is used to show that the chaotic systems of master and slave are remained as it is.

The tested attacked signals on three channels were mostly rejected by the proposed DO. The performance of the proposed DO is given in Figure 6.

At the time of the 3 second, ECG signal was started encrypted and sent. The ECG signal used in the simulation is an array of real numbers with values from -1 to 1 representing the amplitude of the heart rate. The sent ECG signal and received signals are mostly identical. The y-axis of MSSs was used for encryption and decryption by in period of 10s is shown in Figure 7a, which can be seen more clearly in Figure 7b. The encrypted signal is shown in Figure 7c.

To show the correction masking method, the histogram of the sent signal and encrypted signal are given in Figure 8.

Therefore, the proposed control method for secure communication system is good for synchronizing master and slave systems. For enhanced clarity, a comparative analysis is conducted on the histogram charts of the encrypted signal and the sent signal in Fig. 8. The proposed DO can archive the good performance of disturbance rejection. The difference value between sent and received data is zero. To verify the correction and effectiveness of the proposed methods for the secure communication system, the experimental study on chip is given.

B. EXPERIMENTAL STUDY

Herein, the experimental study by using heart rate sensor and two NodeMCU Esp8266 chips was used to conduct the effectiveness of the proposed SCS system. The heart rate sensor in this paper is commercial sensor. Experimental setup is shown in Figure 9.

Heart rate sensor recorded the values corresponding to the amplitude of the ECG signal. Esp8266 chip as the master system read the value from the sensor, then encrypted and sent it to the other Esp8266 as slave system through wireless communication. The sent and received ECG signals were displayed on the computer as monitor. The parameters of the proposed control scheme in the experimental study are as follows: total time $t = 5s$ with time step $h = 0.001s$; The initial states of master chaotic system are $x_m(0) = 0.15, y_m(0) = 0.25, z_m(0) = -0.5$; The initial states of slave chaotic system are $x_s(0) = -1, y_s(0) = -2, z_m(0) = 4$; The damping coefficients of SMC: $\lambda_x = 0.5, \lambda_y = 0.5, \lambda_z = 0.5$; The initial reaching gain of SMC: $k_x = 30, k_y = 30, k_z = 80$; The initial gain of DO: $k_{dx} = 0.1, k_{dy} = 0.1, k_{dz} = 0.1$. First, the states of MSSs are shown in Figure 10.

In Figure 11, the tracking errors are displayed, which are all small. The settling time of three axis are approximately 0.015s. After stabilization, maximum error value is 1.7×10^{-2} when the simulated disturbance is just applied and quickly converge to zero.

To show the maintenance the chaos characteristics after synchronized control design, the phases are shown in Figure 12.

To show the correction of the proposed SCS system, the ECG signal is encrypted and sent from the master to the slave are. The performance of the encrypted and decrypted by using the 10 times of y_m and 10 times of y_s is shown in Figure 14.

As shown in the Figure above, the effectiveness of the proposed control method for the SCS is good for securing the heart rate signal.

V. CONCLUSION

This paper proposed a numerical methods to support the synchronization control of two nonidentical chaotic system, which was used for implementing the encryption and decryption the ECG data on chips. Simultaneously, an adaptive SMC and an adaptive DOB are presented to minimize the errors. Especially, in this paper the ECG signal is also secured in wireless communication system with support of ESP 8266 devices. The experimental study is a huge suggestion for the secure communication of the wireless data transmission protocol based on the chaotic systems for the medical care. In the next, a new application of health care signal with secure communication on chips will be presented.

REFERENCES

[1] D. Murillo-Escobar, C. Cruz-Hernández, R. M. López-Gutiérrez, and M. A. Murillo-Escobar, "Chaotic encryption of real-time ECG signal in embedded system for secure telemedicine," *Integration*, vol. 89, pp. 261–270, Mar. 2023.

[2] C. Song, K. Liu, X. Zhang, L. Chen, and X. Xian, "An obstructive sleep apnea detection approach using a discriminative hidden Markov model from ECG signals," *IEEE Trans. Biomed. Eng.*, vol. 63, no. 7, pp. 1532–1542, Jul. 2016.
[3] D. W. Jung, S. H. Hwang, Y. J. Lee, D.-U. Jeong, and K. S. Park, "Apnea–Hypopnea index prediction using electrocardiogram acquired during the sleep-onset period," *IEEE Trans. Biomed. Eng.*, vol. 64, no. 2, pp. 295–301, Feb. 2017.
[4] X. Wang, Y. Guo, J. Ban, Q. Xu, C. Bai, and S. Liu, "Driver emotion recognition of multiple-ECG feature fusion based on BP network and D–S evidence," *IET Intell. Transp. Syst.*, vol. 14, no. 8, pp. 815–824, Aug. 2020.
[5] M. Al Ameen, J. Liu, and K. Kwak, "Security and privacy issues in wireless sensor networks for healthcare applications," *J. Med. Syst.*, vol. 36, no. 1, pp. 93–101, Feb. 2012.
[6] P. Mathivanan, A. B. Ganesh, and R. Venkatesan, "QR code-based ECG signal encryption/decryption algorithm," *Cryptologia*, vol. 43, no. 3, pp. 233–253, May 2019.
[7] V. N. Giap, Q. D. Nguyen, D. H. Pham, and C.-M. Lin, "Wireless secure communication of chaotic systems based on Takagi–Sugeno fuzzy optimal time varying disturbance observer and sliding mode control," *Int. J. Fuzzy Syst.*, vol. 25, no. 7, pp. 2519–2533, Oct. 2023, doi: 10.1007/s40815-023-01552-8.
[8] S. Çiçek, U. E. Kocamaz, and Y. Uyaroglu, "Secure communication with a chaotic system owning logic element," *AEU-Int. J. Electron. Commun.*, vol. 88, pp. 52–62, May 2018.
[9] V. N. Giap, Q. D. Nguyen, and S.-C. Huang, "Synthetic adaptive fuzzy disturbance observer and sliding-mode control for chaos-based secure communication systems," *IEEE Access*, vol. 9, pp. 23907–23928, 2021, doi: 10.1109/ACCESS.2021.3056413.
[10] N. V. Giap, H. S. Vu, Q. D. Nguyen, and S.-C. Huang, "Disturbance and uncertainty rejection-based on fixed-time sliding-mode control for the secure communication of chaotic systems," *IEEE Access*, vol. 9, pp. 133663–133685, 2021.
[11] M.-Y. Chiang, V. N. Giap, D.-H. Pham, V. L. Nguyen, and S.-C. Huang, "Disturbance observer based on sliding mode control for secure communication of chaotic circuits," *IEEE Access*, vol. 11, pp. 43294–43304, 2023, doi: 10.1109/ACCESS.2023.3272618.
[12] Y.-J. Chen, H.-G. Chou, W.-J. Wang, S.-H. Tsai, K. Tanaka, H. O. Wang, and K.-C. Wang, "A polynomial-fuzzy-model-based synchronization methodology for the multi-scroll Chen chaotic secure communication system," *Eng. Appl. Artif. Intell.*, vol. 87, Jan. 2020, Art. no. 103251.
[13] C.-M. Lin, D.-H. Pham, and T.-T. Huynh, "Synchronization of chaotic system using a brain-imitated neural network controller and its applications for secure communications," *IEEE Access*, vol. 9, pp. 75923–75944, 2021.
[14] C.-M. Lin, D.-H. Pham, and T.-T. Huynh, "Encryption and decryption of audio signal and image secure communications using chaotic system synchronization control by TSK fuzzy brain emotional learning controllers," *IEEE Trans. Cybern.*, vol. 52, no. 12, pp. 13684–13698, Dec. 2022, doi: 10.1109/TCYB.2021.3134245.
[15] B. Vaseghi, S. Mobayen, S. S. Hashemi, and A. Fekih, "Fast reaching finite time synchronization approach for chaotic systems with application in medical image encryption," *IEEE Access*, vol. 9, pp. 25911–25925, 2021.
[16] B. Vaseghi, S. S. Hashemi, S. Mobayen, and A. Fekih, "Finite time chaos synchronization in time-delay channel and its application to satellite image encryption in OFDM communication systems," *IEEE Access*, vol. 9, pp. 21332–21344, 2021.
[17] V. Rybin, T. Karimov, O. Bayazitov, D. Kvitko, I. Babkin, K. Shirnin, G. Kolev, and D. Butusov, "Prototyping the symmetry-based chaotic communication system using microcontroller unit," *Appl. Sci.*, vol. 13, no. 2, p. 936, Jan. 2023.
[18] Z. Lendek, T. Guerra, R. Babuska, and B. D. Schutter, *Stability Analysis and Nonlinear Observer Design Using Takagi–Sugeno Fuzzy Models*. Dordrecht, The Netherlands: Springer-Verlag, 2010.
[19] Q. D. Nguyen, V. N. Giap, D.-H. Pham, and S.-C. Huang, "Fast speed convergent stability of T–S fuzzy sliding-mode control and disturbance observer for a secure communication of chaos-based system," *IEEE Access*, vol. 10, pp. 95781–95790, 2022.
[20] Q. D. Nguyen, Q. D. Pham, N. T. Thanh, and V. N. Giap, "An optimal homogenous stability-based disturbance observer and sliding mode control for secure communication system," *IEEE Access*, vol. 11, pp. 27317–27329, 2023, doi: 10.1109/ACCESS.2023.3257854.
[21] Q. D. Nguyen, S.-C. Huang, and V. N. Giap, "Robust adaptive terminal fixed time sliding-mode control for a secure communication of T–S fuzzy systems," *J. Control, Autom. Electr. Syst.*, vol. 34, no. 3, pp. 507–518, Jun. 2023.
[22] Q. D. Nguyen, D. D. Vu, S.-C. Huang, and V. N. Giap, "Fixed-time supper twisting disturbance observer and sliding mode control for a secure communication of fractional-order chaotic systems," *J. Vibrat. Control*, Jun. 2023, Art. no. 107754632311809.
[23] V. N. Giap, "Text message secure communication based on fractional-order chaotic systems with Takagi–Sugeno fuzzy disturbance observer and sliding mode control," *Int. J. Dyn. Control*, vol. 11, pp. 3109–3123, May 2023.
[24] R. Sakthivel, R. Sakthivel, O. Kwon, and P. Selvaraj, "Synchronisation of stochastic T–S fuzzy multi-weighted complex dynamical networks with actuator fault and input saturation," *IET Control Theory Appl.*, vol. 14, no. 14, pp. 1957–1967, Sep. 2020.
[25] V.-P. Vu, W.-J. Wang, H.-C. Chen, and J. M. Zurada, "Unknown input-based observer synthesis for a polynomial T–S fuzzy model system with uncertainties," *IEEE Trans. Fuzzy Syst.*, vol. 26, no. 3, pp. 1447–1458, Jun. 2018.
[26] Q. Zhang, R. Li, and J. Ren, "Robust adaptive sliding mode observer design for T–S fuzzy descriptor systems with time-varying delay," *IEEE Access*, vol. 6, pp. 46002–46018, 2018, doi: 10.1109/ACCESS.2018.2865618.
[27] V.-N. Giap, S.-C. Huang, Q. D. Nguyen, and T.-J. Su, "Robust control-based disturbance observer and optimal states feedback for T–S fuzzy systems," *J. Low Freq. Noise, Vibrat. Act. Control*, vol. 40, no. 3, pp. 1509–1525, Dec. 2020.
[28] S. Hwang and H. S. Kim, "Extended disturbance observer-based integral sliding mode control for nonlinear system via T–S fuzzy model," *IEEE Access*, vol. 8, pp. 116090–116105, 2020.
[29] W.-H. Chen, D. J. Ballance, P. J. Gawthrop, and J. O'Reilly, "A nonlinear disturbance observer for robotic manipulators," *IEEE Trans. Ind. Electron.*, vol. 47, no. 4, pp. 932–938, Aug. 2000.
[30] X. Wu, K. Xu, M. Lei, and X. He, "Disturbance-compensation-based continuous sliding mode control for overhead cranes with disturbances," *IEEE Trans. Autom. Sci. Eng.*, vol. 17, no. 4, pp. 2182–2189, Oct. 2020.
[31] V. Utkin, "Variable structure systems with sliding modes," *IEEE Trans. Autom. Control*, vol. 22, no. 2, pp. 212–222, Apr. 1997.
[32] C.-K. Chen, C.-L. Lin, C.-T. Chiang, and S.-L. Lin, "Personalized information encryption using ECG signals with chaotic functions," *Inf. Sci.*, vol. 193, pp. 125–140, Jun. 2012.
[33] T.-L. Liao, H.-C. Chen, C.-Y. Peng, and Y.-Y. Hou, "Chaos-based secure communications in biomedical information application," *Electronics*, vol. 10, no. 3, p. 359, Feb. 2021.
[34] D. J. Ewins, S. G. Braun, and S. S. Rao, *Encyclopedia of Vibration, Three-Volume Set*. New York, NY, USA: Elsevier, 2001.
[35] G. Q. Zhong and W. K. S. Tang, "Circuitry implementation and synchronization of Chen's attractor," *Int. J. Bifurcation Chaos*, vol. 12, no. 6, pp. 1423–1427, Jun. 2002.

MINH CHIEN LE is currently pursuing the Engineering degree with the Hanoi University of Science and Technology, Vietnam. His research interests include sliding mode control, disturbance and uncertainty estimation, fuzzy logic control, and secure communication on chips and its applications.

VAN NAM GIAP received the B.S. degree in control engineering and automation from the Hanoi University of Science and Technology, Hanoi, Vietnam, in 2015, the master's degree in electronic engineering from the National Kaohsiung University of Applied Sciences, Kaohsiung, Taiwan, in 2017, and the Ph.D. degree in mechanical engineering from the National Kaohsiung University of Science and Technology, Taiwan, in June 2021. He is currently with the Hanoi University of Science and Technology. His research interests include sliding mode control, disturbance and uncertainty estimation, fuzzy logic control, secure communication, and electric drives control systems.

QUANG DICH NGUYEN received the B.S. degree in electrical engineering from the Hanoi University of Technology, Hanoi, Vietnam, in 1997, the M.S. degree in electrical engineering from the Dresden University of Technology, Dresden, Germany, in 2003, and the Ph.D. degree from Ritsumeikan University, Kusatsu, Japan, in 2010. Since 2000, he has been with the Hanoi University of Science and Technology, where he is currently an Associate Professor and the Executive Dean of the Institute for Control Engineering and Automation. His research interests include magnetic bearings, self-bearing motors, and sensorless motor control.

SHYH-CHOUR HUANG (Senior Member, IEEE) received the bachelor's degree in aeronautics and astronautics engineering from National Cheng-Kung University, Taiwan, in 1980, and the Ph.D. degree in mechanical engineering from the University of Cincinnati, USA, in 1990. He is currently a Professor in mechanical engineering with the National Kaohsiung University of Science and Technology, Taiwan. His research interests include micro-electromechanical systems design, biomechanics, compliant mechanisms, multibody dynamics, fuzzy logic control, vibration control, and optimization algorithms.